Engineering Fracture Mechanics 74 (2007) 771-781
Elsevier Ltd, doi: 101016/j.engfracmech.2006.06.015

A new fracture mechanics theory of orthotropic materials like wood

T.A.C.M. van der Put,
TU-Delft, CiTG, Timber Structures, PO Box 5048, NL-2600 GA Delft, Netherlands
Tel: +31 152851980, *E-mail:* vanderp@xs4all.nl

Abstract
A new, fracture mechanics theory is derived based on a new orthotropic-isotropic transformation of the Airy stress function, making the derivation of the Wu-"mixed mode I - II fracture criterion possible, based on the failure criterion of the flat elliptic crack. As a result of this derivation, the right fracture energy and theoretical relation between mode I and II stress intensities and energy release rates are obtained.

Keywords: Linear elastic fracture mechanics; Mixed mode I-II fracture criterion; flat elliptic crack; fracture energy; energy release rate; orthotropic-isotropic Airy stress-function transformation.

1. Introduction

Fracture mechanics of all materials is now based on the mathematical crack of zero thickness with singularities at the crack tips. This prevents the derivation of the right failure criterion and thus prevents the description of real strength behaviour. This can be corrected by regarding the physical possible flat elliptical crack. Then the mixed mode failure condition can be derived based on the right critical stress state of fracture at the elliptical crack boundary.
Wood and other orthotropic materials should be regarded as reinforced materials. The orthotropic Airy stress function is based on the spread out of the reinforcement to act as a continuum, satisfying the equilibrium, compatibility and strength conditions. In reality this only is possible by interaction through the matrix and the solution thus is not right because the equilibrium conditions and strength criterion of the matrix, as determining element, are not satisfied. It thus is necessary to solve the Airy stress function for the stresses in the isotropic matrix and this appears to give the right solution in accordance with the Wu-failure criterion and other measurements as also is discussed in [1].

Nomenclature

c	= half a crack length
c_{ij}	= constant
E	= elastic modulus
G	= energy release rate or modulus of rigidity
G_C	= critical energy release rate
K, K_C, K_I	= stress intensity factor; c=critical; I mode I
n	= constant
p	= stress
q	= power
r	= radius
s	= power
t	= thickness
$U(z)$, $F(z)$	= stress functions
v	= displacement
x, y; X, Y	= coordinates
z	= $x + iy$, a complex variable
α	= constant
β, θ, δ	= angles
γ	= factor

ε = strain
μ = friction coefficient; root of an equation
ν = Poisson's ratio
ζ = $\xi + i\eta$ complex variable
ξ, η = elliptic coordinates
ξ_0 = boundary of the elliptical crack
σ = normal stress
σ_t = the micro tensile strength of the crack boundary material
τ = shear stress
$\phi(z), \chi(z)$ = stress functions
$\phi(z)$ = stress function

2. Methods of analysis

None of the linear elastic fracture mechanics solutions of the orthotropic Airy stress function are close enough to the measurements to give the real solution. Therefore, the always applied relation between the strain energy release rate G_I and the mode I stress intensity K_I:

$$G_I = K_I^2 \cdot \sqrt{\frac{1}{2E_xE_y}} \cdot \sqrt{\sqrt{\frac{E_x}{E_y}} - \frac{E_x}{2}\left(\frac{2\nu_{xy}}{E_y} - \frac{1}{G_{xy}}\right)} . \tag{1}$$

and the related value of G_{II}, do not apply and are far away from the measurements of e.g. [3]. To correct this, eq.(1) has to be replaced by eq.(2) based on the matrix strength. In eq.(1), G_I is the strain energy release, K_I the mode I stress intensity, and the E 's are the moduli of elasticity and G_{xy} the modulus of rigidity (see e.g. [6], [3]). The reason that eq.(2) and not eq.(1) is determining also follows from the smaller value of G_{Ic} according to eq.(2) showing thus a lower upper bound. Equation (2) follows from the equilibrium and strength conditions of the matrix stresses as follows:
For an elliptic crack of length 2c, in the main direction, in an infinite medium of thickness t, the energy, to open or to close of the crack to an opening "2v", by a stress σ perpendicular to the crack plane, is:
$\frac{\sigma}{2}\pi cvt = \frac{\sigma}{2}\pi c\frac{2\sigma c}{E_y}t$, leading to the equilibrium condition:

$$\frac{\partial}{\partial c}\left(\frac{\pi\sigma^2c^2t}{E} - G_c 2ct\right) = 0 \text{, or: } G_c = \frac{\sigma^2\pi c}{E_y} = \frac{K_{Ic}^2}{E_y} , \tag{2}$$

G_c is the fracture energy per unit fracture surface.
For the flat crack problem, solutions of the two-dimensional orthotropic solid apply. The stress-strain relations then are:

$$\varepsilon_x = c_{11}\sigma_x + c_{12}\sigma_y ; \quad \varepsilon_y = c_{12}\sigma_x + c_{22}\sigma_y ; \quad \gamma_{xy} = c_{66}\tau_{xy} . \tag{3}$$

This can be written:

$$\varepsilon_x = \sigma_x / E_x - \upsilon_{21}\sigma_y / E_y ; \quad \varepsilon_y = -\nu_{21}\sigma_x / E_y + \sigma_y / E_y ; \quad \gamma_{xy} = \tau_{xy} / G_{xy}$$

The Airy function follows from: $\sigma_x = \frac{\partial^2 U}{\partial y^2}$; $\sigma_y = \frac{\partial^2 U}{\partial x^2}$; $\tau_{xy} = -\frac{\partial^2 U}{\partial x \partial y}$,

satisfying the equilibrium equations: $\frac{\partial \sigma_x}{\partial x} + \frac{\partial \tau}{\partial y} = 0$, etc.

Substitutions of eq.(3): $\varepsilon_x = c_{11}\frac{\partial^2 U}{\partial y^2} + c_{12}\frac{\partial^2 U}{\partial x^2}$, etc. in the compatibility condition:

$$\frac{\partial^2\varepsilon_x}{\partial y^2}+\frac{\partial^2\varepsilon_y}{\partial x^2}=\frac{\partial^2\gamma_{xy}}{\partial x\partial y}, \tag{4}$$

gives: $$c_{22}\frac{\partial^4 U}{\partial x^4}+\left(c_{66}+2c_{12}\right)\frac{\partial^4 U}{\partial x^2\partial y^2}+c_{11}\frac{\partial^4 U}{\partial y^4}=0 \tag{5}$$

The general solution of eq.(5) is: $U=\sum_{i}^{4}F_i\left(x+\mu y\right)$, where μ is a root of the characteristic equation:
$c_{11}\mu^4+(c_{66}+2c_{12})\mu^2+c_{22}=0$, giving:

$$\mu^2=\frac{c_{66}+2c_{12}}{2c_{11}}\cdot\left(-1\pm\sqrt{1-\frac{4c_{22}c_{11}}{\left(c_{66}+2c_{12}\right)^2}}\right), \tag{6}$$

thus 4 imaginary roots. Introducing the complex variables z_1 and z_2, defined by: $z_1=x+\mu_1 y\equiv x'+iy'$ and $z_2=x+\mu_2 y\equiv x''+iy''$, the solution of eq.(5) assumes the form:
$U=F_1(z_1)+F_2(z_2)+\bar{F}_1(z_1)+\bar{F}_2(z_2)$,
where the bars denote complex conjugate values. The stresses, displacements and boundary conditions now can be written in the general form of the derivatives of these functions. There are standard methods to solve some boundary value problems (e.g. by Fourier transforms of equations of the boundary conditions) but in principle, these functions have to be chosen, for instance as polynomials, Fourier series or power series in: z or z^{-1}, etc.
For the crack tip problem in orthotropic wood, eq.(5) is chosen in the form:

$$\left(\frac{\partial^2}{\partial x^2}+\alpha_1\frac{\partial^2}{\partial y^2}\right)\left(\frac{\partial^2}{\partial x^2}+\alpha_2\frac{\partial^2}{\partial y^2}\right)U=0 \tag{7}$$

where $\alpha_1\alpha_2=c_{11}/c_{22}$ and $\alpha_1+\alpha_2=\left(c_{66}+2c_{12}\right)/c_{22}$. Introducing 3 sets of polar coordinates for this case, $x+iy=re^{i\theta}$, $x+iy/\sqrt{\alpha_1}=re^{i\theta_1}$, $x+iy/\sqrt{\alpha_2}=re^{i\theta_2}$,
it may be verified that eq.(7) has elementary solutions of the forms:
$r_1^{\pm n}\cos(n\theta_1)$, $r_1^{\pm n}\sin(n\theta_1)$, $r_2^{\pm n}\cos(n\theta_2)$, $r_2^{\pm n}\cos(n\theta_2)$,
as well as terms in $\ln(r_1)$, $\ln(r_2)$. Solutions may be chosen in the form of series of these types. For wood, the powers of r terms were chosen e.g. in [9], what may lead to:

$$\left\{\sigma_r,\sigma_\theta,\sigma_{r\theta}\right\}=\frac{K_A}{(2\pi r)^s}\left\{f_1(\theta),f_2(\theta),f_3(\theta)\right\} \tag{8}$$

and: $$\left\{\sigma_r,\sigma_\theta,\sigma_{r\theta}\right\}=\frac{K_B}{(2\pi r)^q}\left\{f_1(\theta),f_2(\theta),f_3(\theta)\right\} \tag{9}$$

with $q \le s$. This applies only in the vicinity of a notch root as stress singularity at r = 0. Because for $q < s$, the stresses of eq.(8) are always larger than those of eq.(9), the solution, eq.(9), should be rejected based on the boundary conditions at failure. It thus should not have been mentioned that there are 2 singular stress fields, only eq.(8) applies and, as appears, only as approximate solution for the loading case of uniaxial stress in the main direction.
In literature, different values of the power “s” of this power law approximation are given depending on the adjustment. For instance, one finite element solution showed: s = 0.45, near a rectangular notch, while another investigation of the same problem showed values of s = 0.45 for σ and s = 0.10 for τ while s = 0.5 for all stresses according to a boundary collocation method. By the finite difference method, powers are found of s = 0.437 for the same rectangular notch of 90^0 while s = 0.363 and 0.327 for wider notch angles of 153^0 and 166^0. This differs from the test values of s = 0.48, 0.32 and 0.23 for these cases, which are precisely explained by the volume effect according to the new theory (see the next paper that now is under review)
These results show that orthotropic failure is not determining. Because wood is a reinforced material where the reinforcement interacts through the matrix and also the primary cracking is in the matrix, the

failure condition should be based on the strength of the matrix and the Airy stress function of the matrix-stresses should be solved. Lignin is isotropic and hemicellulose and cellulose are transversely isotropic, what means that only one stiffness factor in the main direction has a n-fold higher stiffness in proportion to the higher stiffness of the reinforcement with respect to the matrix stiffness. For a material, with a shear-reinforcement and a tensile reinforcement in the main direction, eq.(10) applies for equilibrium of the matrix stresses:

$$\frac{\sigma_x}{n_1} = \frac{\partial^2 U}{\partial y^2}; \quad \sigma_y = \frac{\partial^2 U}{\partial x^2}; \quad \frac{\tau_{xy}}{n_6} = -\frac{\partial^2 U}{\partial x \partial y}, \tag{10}$$

In stead of using the matrix stresses and the matrix stiffness, the n-fold higher total stresses and n-fold higher stiffness can be used what gives the same compatibility condition, (thus the same condition for the matrix and reinforcement). Inserting the total stresses in the compatibility equation, eq.(4), now gives:

$$c_{22}\frac{\partial^4 U}{\partial x^4} + \left(n_6 c_{66} + (1+n_1)c_{12}\right)\frac{\partial^4 U}{\partial x^2 \partial y^2} + n_1 c_{11}\frac{\partial^4 U}{\partial y^4} = 0 \tag{11}$$

For the isotropic matrix is: $n_1 c_{11} / c_{22} = 1$ and $(n_6 c_{66} + (1+n_1)c_{12})/c_{22} = 2$ giving:

$$\frac{\partial^4 U}{\partial x^4} + 2\frac{\partial^4 U}{\partial x^2 \partial y^2} + \frac{\partial^4 U}{\partial y^4} = \nabla^2(\nabla^2 U) = 0 \tag{12}$$

and: $$n_1 = \frac{c_{22}}{c_{11}} = \frac{E_x}{E_y}; \quad n_6 = \left(2 - \frac{c_{12}}{c_{22}} - \frac{c_{12}}{c_{11}}\right) \cdot \frac{c_{22}}{c_{66}} = \left(2 + \nu_{21} + \nu_{12}\right) \cdot \frac{G_{xy}}{E_y} \tag{13}$$

This orthotropic-isotropic transformation of the Airy stress function and calculation method based on the matrix stresses is used in the following.

3. Theory of fracture mechanics based on the elliptical flat crack

3.1. Introduction.

Because there is a volume effect of the strength and no clear influence on macro-crack propagation of the crack geometry and sharpness of the crack-tip of the notches in wood, orthotropic fracture mechanics is not determining. Determining are the small cracks in the matrix around the macro tip that have to propagate to extend the macro crack and are determining for the total behaviour. This determining small crack behaviour also follows from the failure criterion for combined shear and normal force in common (un-notched) clear wood [7] that is the same as the fracture mechanics criterion eq.(29), for notched wood. It also follows from the simulation of the load-deformation response from randomized weak spots (e.g. small cracks) of test specimens and also follows from the explanation of the volume effect for that case (see Appendix B of [1]).
When "flow" occurs around the crack tip, the ultimate strain condition at the crack- boundary determines the extension of the flow area. The elastic-plastic boundary then acts as an enlarged crack boundary with the "flow" stress as ultimate elastic stress for the linear elastic fracture mechanics calculation..

3.2. Basic equations of the stressed infinite region with an elliptic hole

The classical way of analyzing the elliptic crack problem is to use complex variables and elliptic coordinates.
The Airy stress function can be expressed in terms of two analytic functions of the complex variable z (= x + iy) and the transformation to elliptic coordinates in Fig. 1, gives:
$z = x + iy = c \cdot \cosh(\xi + i\eta)$ or: $x = c \cdot \cosh(\xi) \cdot \cos(\eta)$; $y = c \cdot \sinh(\xi) \cdot \sin(\eta)$.
For an elliptic hole, $\xi = \xi_0$, in an infinite region with uniaxial stress p at infinity in a direction inclined at β to the major axis Ox of the ellipse, the Airy stress function U, satisfying $\nabla^2(\nabla^2 U) = 0$, and satisfying

the conditions at infinity and at the surface $\xi = \xi_0$, showing no discontinuity of displacement, thus being the solution, is: $U = R\{z\phi(z) + \chi(z)\}$, with [2]:

$$4\phi(z) = p\cdot c\cdot \exp(2\xi_0)\cdot\cos(2\beta)\cdot\cosh(\zeta) + p\cdot c\cdot(1 - \exp(2\xi_0 + 2i\beta)\cdot\sinh(\zeta) \tag{14}$$

$$4\chi'(z) = - p\cdot c\cdot[\cosh(2\xi_0) - \cos(2\beta) + \exp(2\xi_0)\cdot\sinh(2\{\zeta - \xi_0 - i\beta\})]\cdot \mathrm{cosech}(\zeta) \tag{15}$$

where $\zeta = \xi + i\eta$.

For the stresses at the boundary, due to a stress p at an angle β to the crack, is:

$$\sigma_\eta - \sigma_\xi + 2i\tau_{\xi\eta} = 2[\bar{z}\varphi''(z) + \chi''(z)]e^{i\delta} \quad \text{and:} \tag{16}$$

$$\sigma_\xi + \sigma_\eta = 2[\varphi'(z) + \overline{\varphi'(z)}] = 4R\{\varphi'(z)\} \tag{17}$$

and the tangential stress σ_t at the surface $\xi = \xi_0$ is simply known from eq.(17) because here $\sigma_\xi = 0$.

Thus:

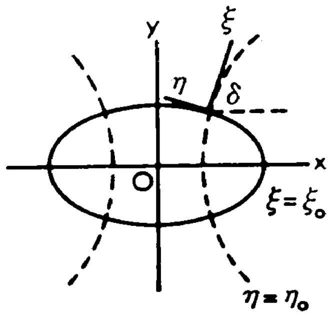

Figure 1 - Elliptic coordinates and elliptic hole.

$$\sigma_t = 2[\varphi'(\xi_0 + i\eta) + \varphi'(\xi_0 - i\eta)] = \frac{p(\sinh(2\xi_0) + \cos(2\beta) - \exp(2\xi_0)\cdot\cos(2(\beta - \eta))}{\cosh(2\xi_0) - \cos(2\eta)} \tag{18}$$

while eq.(15) has to vanish at: $\xi = \xi_0$.

Eq.(18) can be extended for two mutual perpendicular principal stresses p_1 and p_2 (see Fig. 3) by a simple addition leading to eq.(25) below.

3.3. Ideal flat crack solutions

The limit case of the elliptical crack with ξ_0 approaching zero should be comparable with the mathematical flat crack approach of the singularity method, making a comparison of the methods possible. For stresses near the tip of a flat crack, it is possible to choose new coordinates X, Y with the origin in the focus of the ellipse and because ξ and η are small, higher powers than the square can be neglected (see Fig. 2). Thus: $X = x - c = c(\xi^2 - \eta^2)/2$, $\quad Y = y = c\xi\eta$ (19)

or in polar coordinates: $r = \left(X^2 + Y^2\right)^{0.5}$, $X = r\cdot\cos(\theta)$, $Y = r\cdot\sin(\theta)$

and from eq.(19): $\xi^2 + \eta^2 = 2\left(X^2 + Y^2\right)^{0.5}/c = 2r/c$

$$\xi = \sqrt{2r/c}\cdot\cos\left(\theta/2\right), \qquad \eta = \sqrt{2r/c}\cdot\sin\left(\theta/2\right) \tag{20}$$

$$\eta/\xi = \tan\left(\theta/2\right) = \tan\left(\delta\right)$$

Using these relations in the solutions of eq.(16) and (17) the following stresses are found in polar coordinates for the loading case of a stress p at infinity at an angle β with the crack:

$$\left(8r/cp^2\right)^{0.5}\sigma_r = \sin(\theta/2)\left(1-3\sin^2(\theta/2)\right)\sin(2\beta)+2\cos(\theta/2)\left(1+\sin^2(\theta/2)\right)\sin^2(\beta)$$
$$\left(8r/cp^2\right)^{0.5}\sigma_\theta = -3\sin(\theta/2)\cos^2(\theta/2)\sin(2\beta)+2\cos^3(\theta/2)\sin^2(\beta) \quad (21)$$
$$\left(8r/cp^2\right)^{0.5}\tau_{r\theta} = \cos(\theta/2)\left(3\cos^2(\theta/2)-2\right)\sin(2\beta)+2\cos^2(\theta/2)\sin(\theta/2)\sin^2(\beta)$$

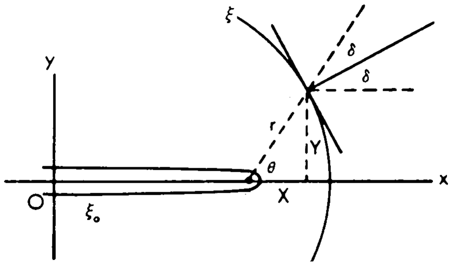

Figure 2 - Confocal coordinates

showing the stress increase by $1/\sqrt{r}$ near the crack tip.
Of interest for the singularity method of wood, is the small crack in the weak direction that only is supposed to propagate in this direction. Then θ= 0 and the equations (21) become:

$$\left(8r/cp^2\right)^{0.5}\sigma_r = 2\sin^2(\beta) \quad (22)$$

$$\left(8r/cp^2\right)^{0.5}\sigma_\theta = 2\sin^2(\beta) \quad (23)$$

$$\left(8r/cp^2\right)^{0.5}\tau_{r\theta} = 2\sin(\beta)\cos(\beta) \quad (24)$$

These equations simply give the Rankine, or the maximum stress conditions of the strengths in the main planes. Thus fracture occurs when the tensile strength is reached perpendicular to the grain and/or when the shear strength in this plane is reached. Thus: $K_I \le K_{Ic}$ and $K_{II} \le K_{IIc}$ for all stress states (without interaction). It is known, that this does not apply, showing that the, by the singularity method predicted, critical states are not determining for fracture. This does not only apply for the matrix stresses but also for the applied, n-fold higher orthotropic stresses.
The right failure condition for combined stresses will be derived below.

3.4. Derivation of the "mode I - II" - interaction equation

A general failure criterion [5] follows from the ultimate stress that occurs at the boundary of the crack. By an extension of eq.(18) (by superposition) to $p_1 = \sigma_1$ inclined at an angle π/2 + β to the Ox-axis and $p_2 = \sigma_2$ inclined at an angle β, (see Fig. 3), eq.(18) turns to:

$$\sigma_t = \frac{2\sigma_y \sinh(2\xi_0) + 2\tau_{xy}[(1+\sinh(2\xi_0))\cdot\cot(2\beta) - \exp(2\xi_0)\cdot\cos(2(\beta-\eta))\,\mathrm{cosec}(2\beta)]}{\cosh(2\xi_0)-\cos(2\eta)},$$

where the stresses are given in crack coordinates with the x-axis along the crack. For small values of ξ_0 and η (flat cracks), this equation becomes:

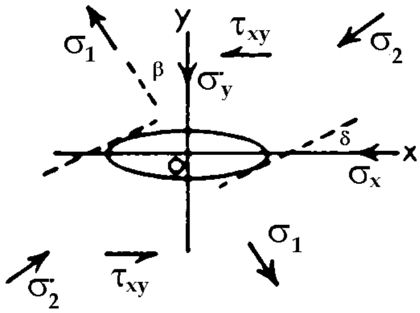

Figure 3 - Stresses in the crack plane Ox

$$\sigma_t = \frac{2\left(\xi_0\sigma_y - \eta\tau_{xy}\right)}{\xi_0^2 + \eta^2} \tag{25}$$

The maximum (critical) value of the tangential stress σ_t, depending on η, is found by: $d\sigma_t / d\eta = 0$, giving the critical value of η:

$$-2\tau_{xy} / \left(\xi_0^2 + \eta^2\right) - \left(2\left(\xi_0\sigma_y - \eta\tau_{xy}\right)\cdot 2\eta\right) / \left(\xi_0^2 + \eta^2\right)^2 = 0, \text{ or:}$$

$$-\tau_{xy}\left(\xi_0^2 + \eta^2\right) = 2\eta\left(\xi_0\sigma_y - \eta\tau_{xy}\right) = \eta\sigma_t\left(\xi_0^2 + \eta^2\right)$$

where in the last equation, the second equality sign is due to the substitution of eq.(25). From the first and last term of this equation follows that: $\eta\sigma_t = -\tau_{xy}$ and from the first 2 terms:

$$\eta / \xi_0 = \left(\sigma_y \pm \sqrt{\sigma_y^2 + \tau_{xy}^2}\right) / \tau_{xy} \tag{26}$$

or with eq.(25):

$$\xi_0\sigma_t = \sigma_y \pm \sqrt{\sigma_y^2 + \tau_{xy}^2} \tag{27}$$

and eq.(27) can be written:

$$1 = \frac{\sigma_y}{\xi_0\sigma_t / 2} + \frac{\tau_{xy}^2}{\xi_0^2\sigma_t^2} \tag{28}$$

According to eq.(20) is, for a small value of θ: $\xi_0 = \sqrt{2r_0 / c}$, giving in eq.(28):

$$1 = \frac{\sigma_y\sqrt{\pi c}}{\sigma_t\sqrt{2\pi r_0} / 2} + \frac{\left(\tau_{xy}\sqrt{\pi c}\right)^2}{\left(\sigma_t\sqrt{2\pi r_0}\right)^2}$$

what is identical to the empirical parabolic interaction equation of Wu:

$$\frac{K_I}{K_{Ic}} + \frac{\left(K_{II}\right)^2}{\left(K_{IIc}\right)^2} = 1 \tag{29}$$

For an isotropic material, crack propagation starts at the worst oriented initial cracks, depending on the stress state, that can be found by equating: $d\sigma_t / d\beta = 0$ in eq.(18). For wood, the presence of such worst oriented cracks will lead to the early crack formation in the weak direction, along the grain, that will act as the initial cracks for later failure. Nearly isotropic behaviour of the matrix with initial cracks in the weak planes along the grain occurs in Balsa wood, as follows from $K_{IIc} = 2K_{Ic}$, according to eq.(28) and (29) in accordance with the measurements of Wu on Balsa being $K_{IIc} \approx 140\,\text{psi}\cdot\text{in}^{0.5}$ and $K_{Ic} \approx 60\,\text{psi}\cdot\text{in}^{0.5}$.

Eq.(29) is generally applicable also when σ_y is a compression stress as follows from the measurements of Figure 4. When the compression is high enough to close the small cracks ($\sigma_{y,cl} \approx 2G_{xy}\xi_0$), τ_{xy} has to be replaced by the effective shear stress: $\tau^*_{xy} = \tau_{xy} + \mu\left(\sigma_y - \sigma_{y,cl}\right)$ in eq.(28) or:

$$1 = \frac{\sigma_{y,cl}}{\xi_0\sigma_t/2} + \frac{\left(\tau^*_{xy}\right)^2}{\xi_0^2\sigma_t^2}, \qquad (30)$$

what is fully able to explain fracture by compression perpendicular to the crack plane (see Fig. 4). In this equation is μ the friction coefficient.

For species, with denser layers than those of Balsa, a much higher value of K_{IIc} than twice the value of K_{Ic} is measured because due to the reinforcement, η is smaller than the isotropic critical value of eq.(26). To read the equation in applied stress values, the matrix stress τ_{iso} has to be replaced by τ_{ort}/n_6 in eq.(26), and the slope δ in Fig. 2 of the location of the failure stress, is: $\tan\delta = \eta_m/\xi_0 = 1/2n_6$.

For small values of $\eta = -|\eta|$, eq.(25) can be written, neglecting $(\eta/\xi_0)^2$:

$$\frac{\sigma_y}{\xi_0\sigma_t/2} = 1 + \frac{\eta^2}{\xi^2} - \frac{\tau_{xy}}{\xi_0^2\sigma_t/\left(2|\eta|\right)} \approx 1 - \frac{\tau_{xy}}{\xi_0^2\sigma_t/\left(2|\eta|\right)}$$

where $|\eta|$ is the absolute value of η, being negative. Thus:

$$\frac{K_I}{K_{Ic}} + \frac{K_{II}}{K_{IIc}} \approx 1 \qquad (31)$$

This is a lower bound, with: $K_{IIc} = \left(\xi_0/|\eta_m|\right)\cdot K_{Ic}$ (32)

and the maximal value of $\eta = \eta_m$ is found by measuring K_{Ic} and K_{IIc}, giving e.g. a value of about $\xi_0/\eta_m \approx 7.7$, showing that the neglect of $\left(\eta/\xi_0\right)^2$ = 0.017 with respect to 1 is right. Measurements between the lines eq.(29) and (31) thus indicate a strong difference between K_{IIc} and K_{Ic} of the structure that is crossed by the propagating crack.

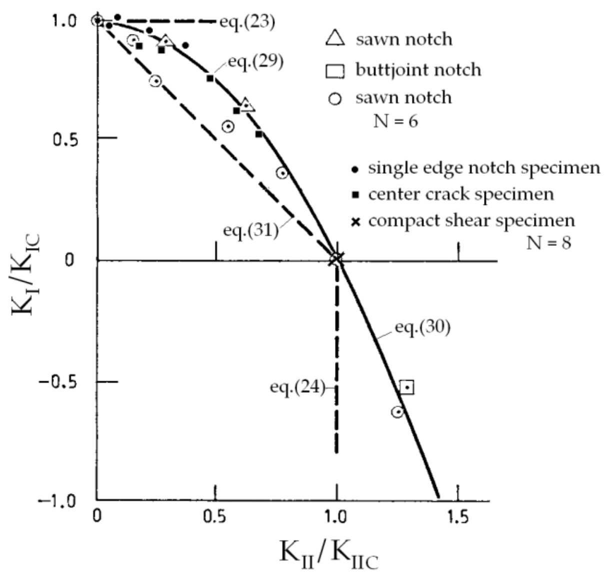

Figure 4 - Fracture strength under combined stresses [4], [6]

Thus far, the equations are given in matrix stresses. To change this in the real applied orthotropic stresses, $\tau_{iso} = \tau_{ort}/n_6$ has to be inserted in eq.(28) giving:

$$1 = \frac{\sigma_y}{\xi_0\sigma_t / 2} + \frac{\tau_{iso}^2}{\xi_0^2\sigma_t^2} = \frac{\sigma_y}{\xi_0\sigma_t / 2} + \frac{\tau_{ort}^2}{\xi_0^2\sigma_t^2 n_6^2} = \frac{K_I}{K_{Ic}} + \frac{\left(K_{II}\right)^2}{\left(K_{IIc}\right)^2} \tag{33}$$

and it follows that: $\frac{K_{IIc}}{K_{Ic}} = \frac{\xi_0\sigma_t n_6}{\xi_0\sigma_t / 2} = 2n_6$ (34)

according to eq.(13) is e.g. for small clear specimens:
$2n_6 = 2\cdot\left(2+\nu_{21}+\nu_{12}\right)\cdot(G_{xy}/E_y)$ = 2(2 + 0.57)/0.67 = 7.7 for Spruce
and: 2(2 + 0.48)/0.64 = 7.7 for Douglas Fir in TL-direction.
This is independent of the densities of respectively 0.37 and 0.50 at a moisture content of 12 %. Thus, for $K_{Ic} \approx 265\,\mathrm{kN/m^{1.5}}$ is $K_{IIc} = 7.7\cdot 265 = 2041\ \mathrm{kN/m^{1.5}}$ in the TL-direction. This agrees with measurements [6]. In RL-direction this factor is 3.3 to 4.4. Thus, when K_{IIc} is the same as in the TL-direction, the strength in RL-direction is predicted to be a factor 1.7 to 2.3 higher with respect to the TL-direction. This however applies at high crack velocities (“elastic” failure) and is also dependent on the site of the crack. At common loading rates a factor lower than 410/260 = 1.6 is measured [6] and at lower crack speeds, this strength factor is expected to be about 1 when fracture is in the “isotropic” middle lamella. It then thus is independent of the TL and RL-direction according to the local stiffness and rigidity values. To know the mean influence, it is necessary to analyze fracture strength data dependent on the density and the elastic constants of n_6. From the rate dependency of the strength follows an influence of viscous and viscoelastic processes. This has to be analyzed by deformation kinetics (see [8] and [1]-Rheology).
A general problem is further the possible early instability of the mode I-tests. This means that small crack instability outside the crack-tip is determining e.g. in the tests of [6] (see [1]). In this case all constants should be related to the mode II data.

3.5. Experimental verification

Measurements are given in fig. 4. The points are mean values of series of 6 or 8 specimens. The theoretical line eq.(29) is also the mean value of the extended measurements of Wu on balsa plates. Only the Australian sawn notch data deviate from this parabolic line and lie between eq.(29) and the theoretical lower bound eq.(31). This is explained by the theory by a too high K_{IIc}/K_{Ic}-ratio, indicating a mistake in manufacture. The theoretical prediction that $K_{IIc} = 2K_{Ic}$, for dominant isotropic behaviour of the matrix, is verified for Balsa with its extremely low fiber density. The prediction that K_{IIc}/K_{Ic} $= 2\cdot\left(2+\nu_{21}+\nu_{12}\right)\cdot(G_{xy}/E_y)$ agrees with the measurements, using general mean values of the constants. However, precise, local values of the constants at the cracks are not measurable and there is an influence of the loading rate and cracking speed. Thus safe lower bound values have to be used in practice.
The theory also fully explains the influence of compression perpendicular to the crack plane on the shear strength, eq.(30) in fig. 4.
The conclusion thus is that all measurements are explained by the theory.

4. Energy Principle

4.1. Correction of the Energy Equation.

Eq.(2) can be extended by superposition to:

$$\sigma_y^2 + \tau_{xy}^2 = G_f E_y / \pi c \tag{35}$$

This only is right, when G_f is not constant but depends on σ_y / τ_{xy}, because else, for σ_y = 0, eq.(35) predicts a too low shear strength. This already was noticed by Griffith. The equilibrium method gives a two times higher shear strength than according to the energy method. This was explained by supposing that there is plenty of energy for failure, but that the shear stresses are too low for failure. This means that the failure condition eq.(33) is determining for G_f in the energy equation.

For the orthotropic case eq.(35) is: $\sigma_y^2 + \tau_{xy}^2 / n_6^2 = G_f E_y / \pi c$ and when $\tau_{xy} = 0$, is $G_f = G_{Ic}$ and $K_{Ic} = \sqrt{E_y G_{Ic}}$. When $\sigma_y = 0$ is: $\tau_{xy}^2 \pi c = n_6^2 G_{IIc} E_y = 4 n_6^2 G_{Ic} E_y$, because $K_{IIc} = 2 n_6 K_{Ic}$ (eq,(34)). Thus: $K_{IIc} = n_6 \sqrt{E_y G_{IIc}} = 2 n_6 \sqrt{E_y G_{Ic}}$ or: $G_{IIc} = 4 G_{Ic}$

The failure condition eq.(33) can be written in fracture energies:

$$\frac{K_I}{K_{Ic}} + \frac{(K_{II})^2}{(K_{IIc})^2} = 1 = \frac{\sqrt{G_I}}{\sqrt{G_{Ic}}} + \frac{G_{II}}{G_{IIc}} = \frac{\sqrt{\gamma \cdot G_f}}{\sqrt{G_{Ic}}} + \frac{(1-\gamma) \cdot G_f}{G_{IIc}} \tag{36}$$

where: $G_f = G_I + G_{II} = \gamma \cdot G_f + (1-\gamma) \cdot G_f$

$$\text{Thus: } \frac{\gamma G_f}{(1-\gamma) G_f} = \frac{K_I^2}{K_{II}^2} \text{ or: } \gamma = \frac{1}{1 + \frac{K_{II}^2}{K_I^2}} = \frac{1}{1 + \frac{\tau_{xy}^2}{\sigma_y^2 \eta_6^2}} \tag{37}$$

and γ depends on the critical stress combination τ_{xy} / σ_y for the small cracks near the macro crack-tip at failure and not on the stresses of the fracture energy.

Eq.(36) is a quadratic equation in $\sqrt{\gamma G_f / G_{Ic}}$ and the real root is:

$$\sqrt{\frac{\gamma \cdot G_f}{G_{Ic}}} = \frac{G_{IIc}}{2G_{Ic}} - \frac{G_{IIc}}{2G_{Ic}} \cdot \sqrt{1 - \frac{4G_{Ic}}{G_{IIc}} + \frac{4G_{Ic}G_f}{G_{IIc}^2}} = \frac{K_I}{K_{Ic}} \tag{38}$$

Measuring $G_f = G_c$ and knowing G_{IIc} / G_{Ic}, γ can be calculated providing the best estimate of the determining stress combination of shear τ_{xy} with tension perpendicular σ_y of a given structure or notch type.

Eq.(38) can be written: $G_f = 4G_{Ic} / (1 + \sqrt{\gamma})^2 = G_{IIc} / (1 + \sqrt{\gamma})^2$ (39)

when the theoretical value $G_{IIc} / G_{Ic} = 4$ applies.

Applications of the theory with the total critical fracture energy G_f, depending on the type of structure, are given in [1].

4.2. Experimental confirmation.

The theory is e.g. applied for beams with rectangular end notches as basis of the design rules of the Dutch Timber Structures Code and some other Codes and is a correction of the method of the Euro-Code.

In the Euro-Code, an approximate compliance difference is used and a raised stiffness according eq.(1). Further G_{Ic} is used in stead of G_f according to eq.(39). It appears however, also from other testing as in [3], that eq.(2) has to be applied in stead of eq.(1) and the calculation has to based on the real compliances. Use of G_f according eq.(39) explains the differences in fracture energies depending on the notch depth and structure and shear slenderness of the beam by the different occurring τ_{xy} / σ_y-values according to eq.(37).

Important is further that the theoretical prediction $G_{IIc} = 4G_{Ic}$ is verified by measuring G_{IIc} / G_{Ic} = 3.5 (R^2 = 0.64).

At comparing results it should be realized that there is Weibull volume effect of the strength [1].

5. Conclusions

- The singularity approach of fracture mechanics, applied to all materials, is not able to give the right fracture criterion for orthotropic materials.
- Based on the elliptical crack approach, the mixed I-II-mode fracture criterion can be derived as consequence of the ultimate tensile strength condition for the uniaxial stress along the micro-crack boundary.
- The critical fracture energy follows from the failure condition of combined stresses due to the critical stress state at the crack boundary of the critical small crack. For every type of notched structure therefore a different apparent critical energy release rate is to be expected independent of the stress combinations of the strain energy. Although for an end notch, in one case, the fracture energy was nearly only shear strain energy, while in an other case there almost only was bending strain energy, there in both cases was a combined failure, mode leading to a value of G_c close to the mode I value and not to mode II value, as is predicted by the other methods.
- Based on this adapted critical energy release rate, a correction of the energy approach for fracture of timber beams with end notches is given in [1] that also can be applied to brittle joints loaded perpendicular to the grain.
- The concept of equilibrium, compatibility and strength requirements of the isotropic matrix stresses provides a simple orthotropic-isotropic transformation of the Airy-stress function.
- Based on this approach is: $K_{Ic} = \sqrt{E_y G_{Ic}}$, $K_{IIc} = n_6 \sqrt{E_y G_{IIc}}$ and $G_{IIc} = 4G_{Ic}$

$G_f = 4G_{Ic} / (1+\sqrt{\gamma})^2 = G_{IIc} / (1+\sqrt{\gamma})^2$ with : $\gamma = 1/\left(1+\tau_{xy}^2 / \sigma_y^2\right)$ and:

$n_6 = \left(2+\nu_{21}+\nu_{12}\right) \cdot \left(G_{xy} / E_y\right)$

- The theory explains the relations between K_{Ic} and K_{IIc} in TL- and in RL-direction that are related by the ultimate strength at the crack boundary depending on the cracked wood-layer material.
- The theoretical value of $G_{IIc} = 4G_{Ic}$ is verified by measurements where ratio 3.5 is found ($R^2 = 0.64$) in stead of 4.
- The verification of the derived theory by measurements shows the excellent agreement. The method provides an exact solution and is generally applicable.

References

[1] van der Put T.A.C.M., A new consistent theory of fracture mechanics of wood. Website: www.dwsf.nl/downloads

[2] Timoshenko S. and Goodier J.N., Theory of elasticity, McGraw-Hill book comp., N.Y. 1951, 179-204.

[3] Bostrom, L., Method for determination of the softening behaviour of wood etc. Thesis, Report TVBM-1012, Lund, Sweden, 1992.

[4] Leicester R.H., Fracture strength of wood, First Australian Conf. on Engin. Materials, Univ. of New South Wales, 1974.

[5] van der Put, T.A.C.M., Explanation of the mixed mode interaction equation, COST 508 workshop 2, papers, Bordeaux, April 1992

[6] RILEM state of the art report on fracture mechanics, Espoo, 1991.

[7] van der Put, T.A.C.M., Explanation of the failure criterion of wood, COST 508 workshop on plasticity and damage, Limerick, Ireland, 1993.

[8] van der Put, T.A.C.M., Deformation and damage processes in wood, Delft University press, 1989.

[9] R.H. Leicester, Design specifications for notched beams in AS 1720, CIB-W18/38-6-1, meeting 38, Karlsruhe, Germany, August 2005.